Theoretical prediction and experimental study of a ferromagnetic shape memory alloy: Ga_2MnNi

S. R. Barman,[1,*] Aparna Chakrabarti,[2] Sanjay Singh,[1] S. Banik,[1] S. Bhardwaj,[1] P. L. Paulose,[3] B. A. Chalke,[3] A. K. Panda,[4] A. Mitra,[4] and A. M. Awasthi[1]

[1]*UGC-DAE Consortium for Scientific Research, Khandwa Road, Indore 452001, India*

[2]*Raja Ramanna Centre for Advanced Technology, Indore 452013, India*

[3]*Tata Institute of Fundamental Research, Mumbai 400005, India*

[4]*National Metallurgical Laboratory, Jamshedpur 831007, India*

(Received 17 May 2008; published 9 October 2008)

We predict the existence of a ferromagnetic shape memory alloy Ga_2MnNi using density-functional theory. The martensitic start temperature (T_M) is found to be approximately proportional to the stabilization energy of the martensitic phase (δE_{tot}) for different shape memory alloys. Experimental studies performed to verify the theoretical results show that Ga_2MnNi is ferromagnetic at room temperature and T_M and T_C are 780 and 330 K, respectively. Both from theory and experiment, the martensitic transition is found to be volume conserving that is indicative of shape memory behavior.

DOI: 10.1103/PhysRevB.78.134406 PACS number(s): 75.50.Cc, 71.15.Nc, 81.30.Kf

I. INTRODUCTION

Ni_2MnGa exhibits both ferromagnetism and shape memory effect and is a promising candidate for technological applications because of its high actuation frequency compared to conventional shape memory alloys.[1] The unusually large strain caused by a moderate magnetic field (10% at 1 T),[1] the observation of giant magnetocaloric effect,[2] and large negative magnetoresistance[3] in Ni_2MnGa have started intense research activity in ferromagnetic shape memory alloys (FSMA). However, a major drawback of Ni_2MnGa is its brittleness. So, the present challenge in FSMA research lies in the search for new materials that have magnetomechanical properties superior to Ni_2MnGa and preferably having high martensitic start temperature (T_M) and Curie temperature (T_C). Recently, different groups have attempted to find FSMA materials with properties superior to Ni_2MnGa. Takeuchi *et al.*[4] have studied a range of compositions in the Ni-Mn-Ga phase diagram and found that the martensitic transition temperature decreases as the magnetization increases. Although martensitic transition and inverse magnetocaloric effect have been reported recently in nonstoichiometric compositions of Ni-Mn-Sn, Ni-Mn-In, and Ni-Co-Mn-In,[5–7] these systems have not emerged as viable alternatives to Ni_2MnGa.

Since related stoichiometric alloys such as Ni_2MnAl, Ni_2MnIn, and Ni_2MnSn do not exhibit martensitic transition,[8] it is apparent that Ga plays an important role in making Ni_2MnGa a shape memory alloy. Substitution of Ga by In in Ni_2MnGa decreases T_M.[9] Thus, excess Ga may have a stabilizing effect on the martensitic phase. Zayak *et al.*[10] theoretically studied the role of Ga $4p$ states in the stability of the martensitic phase of Ni_2MnGa. While considerable experimental work has been done on Ni and Mn excess Ni-Mn-Ga,[11–14] this is not the case for Ga excess Ni-Mn-Ga. Theoretical investigations so far have concentrated on the electronic structure of Ni_2MnGa and related stoichiometric Heusler alloys and total-energy calculations have been done to ascertain the stability of the martensitic phase.[15–20]

Here, using spin-polarized full-potential *ab initio* density-functional theory, we establish a method to estimate the martensitic structural transition temperature and predict possible existence of another FSMA Ga_2MnNi. A tetragonal martensitic phase with $c/a=0.83$ is found to be lower in total energy (E_{tot}) compared to the cubic austenitic phase. The martensitic phase total energy is lower by 55 meV/atom ($=\delta E_{tot}$, i.e., the stabilization energy, which is the difference of E_{tot} between the austenitic and martensitic phases). This value is larger than other FSMA materials studied by us.[20–22] Based on our data and those in Refs. 23 and 24, we show that δE_{tot} is approximately proportional to T_M. E_{tot} for the ferromagnetic state is lower than the paramagnetic state, showing that Ga_2MnNi is ferromagnetic. Inspired by the theoretical prediction, Ga_2MnNi has been prepared and it indeed exhibits a thermoelastic martensitic transition with $T_M=780$ K, which is the highest reported so far in the Ni-Mn-Ga family. T_C is 330 K. X-ray diffraction (XRD) shows that the structure is monoclinic with $b\approx 7a$, indicating the existence of modulation and, hence, the possibility of magnetic-field-induced strain. Both from experiment and theory, we find that there is hardly any unit-cell volume change across the martensitic transition, and this is strongly indicative of shape memory behavior.[25]

II. METHODOLOGY

The *ab initio* relativistic spin-polarized full-potential-linearized-augmented-plane-wave (FPLAPW) method calculations were performed using WIEN97 code[26] with the generalized gradient approximation for exchange correlation. An energy cutoff for the plane-wave expansion of 16 Ry is used ($R_{MT}K_{max}=9$). The cutoff for charge density is $G_{max}=14$. The maximum $l(l_{max})$ for the radial expansion is 10 and for the nonspherical part, $l_{max,ns}=4$. The muffin-tin radii are Ni: 2.2488, Mn: 2.3999, and Ga: 2.2488 a.u. The number of k points for self-consistent field cycles in the irreducible Brillouin zone is 413 and 1063 in the austenitic and martensitic phase, respectively. E_{tot} consists of the total kinetic, potential, and exchange-correlation energies of a periodic solid.[27] The convergence criterion for the total energy E_{tot} is 0.1

mRy, which implies that the accuracy of E_{tot} is ± 0.34 meV/atom. The charge convergence is set to 0.001. The tetrahedron method for the k-space integration has been used.

Polycrystalline ingots of Ga_2MnNi were prepared by melting appropriate quantities of the constituent metals of 99.99% purity in an arc furnace under argon atmosphere and subsequently annealed in sealed quartz ampule wrapped in Mo foil at 873 K for 12 days, then at 723 K for 1 day, and finally slowly cooled to room temperature. The differential scanning calorimetry (DSC) measurements were done by using TA instruments MDSC model 2910 at a scan rate of 10°/min. Magnetization was performed using vibrating sample magnetometers from Oxford Instruments and Lake Shore Cryotronics, Inc. Powder XRD patterns were obtained using Cu $K\alpha$ radiation with Rigaku XRD unit at a scan rate of 2°/min. Energy dispersive analysis of x-rays (EDAX) was done using scanning electron microscope with Oxford detector model with 2% accuracy by estimating the intensities of Ni, Mn, and Ga $K\alpha$ characteristic lines (5.9–9.2 keV) that are well separated and have small background by averaging over several measurements.

III. RESULTS AND DISCUSSION

A. Theoretical studies using FPLAPW method

The positions of the atoms in the cubic austenitic phase of Ga_2MnNi are determined from the E_{tot} calculations in the L_{2_1} cubic structure that consists of four interpenetrating fcc lattices at (0.25,0.25,0.25), (0.75,0.75,0.75), (0.5,0.5,0.5), and (0,0,0) [Figs. 1(a) and 1(b)]. The first two positions are equivalent (8f), whereas the other two are 4a and 4b, respectively. In our notation, GaGaMnNi means that the two Ga atoms occupy (0.25,0.25,0.25) and (0.75,0.75,0.75), i.e., the 8f positions, while Mn and Ni are at (0.5,0.5,0.5) and (0,0,0), respectively. Similarly, GaNiGaMn means that Ga atoms occupy inequivalent (0.25,0.25,0.25) and (0.5,0.5,0.5) positions, while Ni and Mn atoms are at (0.75,0.75,0.75) and (0,0,0), respectively. E_{tot} has been calculated as a function of lattice constant (a) for all the different possible Ga positions (GaGaMnNi, GaGaNiMn, NiMnGaGa, NiGaMnGa, GaNiGaMn, and GaMnGaNi), where the two Ga atoms occupy either symmetry equivalent or inequivalent points. E_{tot} values for the inequivalent Ga structures [NiGaMnGa, GaNiGaMn, and GaMnGaNi; Fig. 1(b)] are similar. The equivalent Ga structures [GaGaMnNi, GaGaNiMn, and NiMnGaGa; Fig. 1(a)] are also very close to each other in energy. The data have been fitted using a least square minimization routine using the Murnaghan equation of state [solid lines, Fig. 1(c)]. The minimum E_{tot} for the equivalent Ga structures (arrow) is lower by 113 meV/atom compared to the inequivalent Ga structure (tick), unambiguously denoting the former to be the stable structure of Ga_2MnNi in the austenitic phase. The E_{tot} minimum (arrow) is at $a=11.285$ a.u. (5.96 Å) with the unit-cell volume of 1437 a.u. (Ref. 3) [Fig. 1(c)]. Furthermore, the formation energy of Ga_2MnNi is calculated by $E_{tot}(Ga_2MnNi)-2E_{tot}(Ga)-E_{tot}(Mn)-E_{tot}(Ni)$. The formation energy turns out to be negative comparable to Ni_2MnGa, indicating that the compound is stable. It should be noted

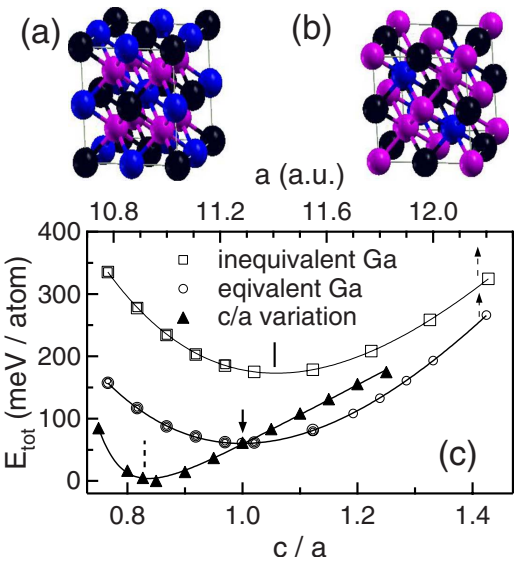

FIG. 1. (Color online) The structure of Ga_2MnNi where (a) Ga atoms occupy equivalent position (GaGaMnNi) and (b) Ga atoms occupy inequivalent positions (NiGaMnGa) in the L_{2_1} austenitic (cubic) phase. The violet (light shading), black, and blue (dark shading) spheres represent Ga, Mn and Ni atoms, respectively. (c) The total energies E_{tot} of Ga_2MnNi as a function of lattice constant a in the austenitic phase for structures with inequivalent and equivalent Ga atoms. E_{tot} as a function of c/a shows how a tetragonal distortion lowers E_{tot}. The dashed arrows indicate the corresponding curves are plotted against the top axis. E_{tot} is plotted with respect to the lowest energy in the martensitic phase that is taken to be zero.

that all the calculations shown in Fig. 1(c) have been performed in the ferromagnetic state since this is the stable magnetic phase (discussed later).

The martensitic transition involves a structural transition from cubic to a lower symmetry phase with decreasing temperature. In order to study this phase transition in Ga_2MnNi, our strategy is to calculate E_{tot} as a function of a volume-conserving tetragonal distortion by varying c/a. As c/a is increased from the cubic value of unity, E_{tot} increases [Fig. 1(c)]. On the other hand, for $c/a<1$, E_{tot} initially decreases and a minimum is obtained at $c/a=0.83$ (dashed tick). In the next step to reach the global E_{tot} minimum in the martensitic phase, the unit-cell volume is varied keeping c/a fixed and the minimum is obtained at the unit-cell volume of 1435.8 a.u. with $a=12.004$ and $c=9.964$ a.u. [Fig. 2(a), dashed arrow]. Thus, although there is a large change in lattice constants (+6.4% in a and −11.7% in c), there is almost no volume change between the austenitic and the martensitic phases. E_{tot} has been calculated for Ga_2MnNi in the paramagnetic state in the martensitic phase using the optimized lattice constants. It turns out to be 156 meV/atom higher than the ferromagnetic state. Thus, Ga_2MnNi has a ferromagnetic ground state. The total spin magnetic moment of Ga_2MnNi in austenitic (martensitic) phase is 3.04 (2.97) μ_B. The local moments of Mn, Ni, and Ga in the austenitic (martensitic) phase are 3.03 (2.87), 0.06 (0.16), and −0.05 (−0.05)μ_B, respectively. On the basis of the condition that a volume-conserving martensitic transition is the necessary and suffi-

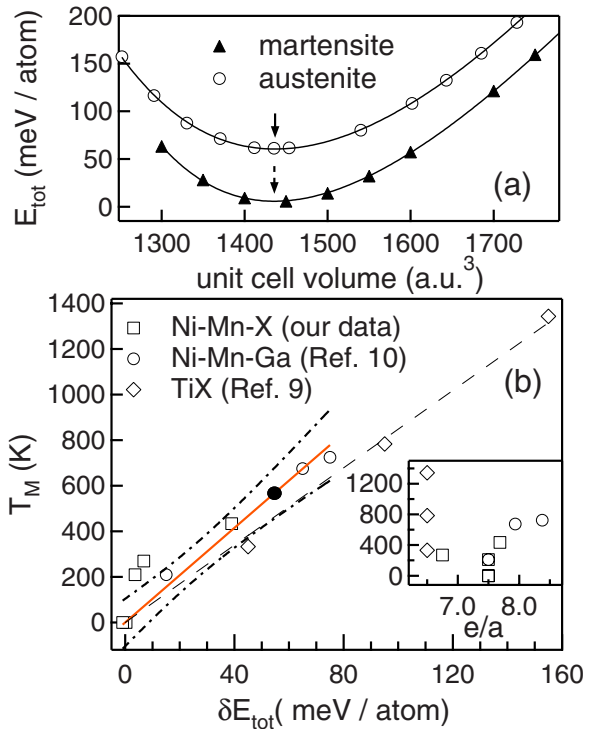

FIG. 2. (Color online) (a) E_{tot} for Ga_2MnNi in the austenitic and martensitic phases as a function of the unit-cell volume. The solid lines are a fit to the data. The minima are shown by arrows. (b) The martensitic transition temperature T_M is plotted against δE_{tot} for Ni_2MnAl, Ni_2MnIn, Ni_2MnGa, Mn_2NiGa, and $Ni_{2.25}Mn_{0.75}Ga$ (our data are shown by squares). $Ni_{8+x}Mn_4Ga_{4-x}$ for $x=0$, 1, and 2 from Ref. 24 (circle) and for TiX with X=Ni, Pd, and Pt from Ref. 23 (diamond). A straight-line fit and the 90% confidence interval for the Ni-Mn-X data (square and circle) are shown by the red solid line and the black dot-dashed lines, respectively. The filled circle on this line shows the theoretically predicted T_M for Ga_2MnNi to be 570 K, corresponding to δE_{tot} of 55 meV/atom. A straight-line fit for TiX is shown by a dashed line. The absence of a correlation between T_M and e/a for the above discussed alloys is shown as an inset.

cient condition for shape memory behavior[25] and that the ground state is ferromagnetic, we predict that Ga_2MnNi will behave as a ferromagnetic shape memory alloy.

The martensitic phase being the lower temperature phase, E_{tot} for the martensitic phase is lower than the austenitic phase by 55 meV/atom. Larger stabilization energy, i.e., δE_{tot} would imply greater stability of the martensitic phase and enhanced T_M. From our earlier calculations, δE_{tot} (experimental T_M) is found to be 3.6 (210 K), 6.8 (270 K), and 39 (434 K) meV/atom for Ni_2MnGa, Mn_2NiGa, and $Ni_{2.25}Mn_{0.75}Ga$, respectively.[20–22,28] Here, we report on similar calculations for Ni_2MnIn and Ni_2MnAl. The optimized lattice constants of Ni_2MnAl and Ni_2MnIn (5.79 and 6.06 Å, respectively) are in good agreement with experiment: 5.83 and 6.08 Å.[29] Although their off-stoichiometric compositions exhibit martensitic transition, it is well known that neither of these Heusler alloys undergo martensitic transition.[8] Interestingly for Ni_2MnIn, δE_{tot} turns out to be almost zero (0.34 meV/atom) within the theoretical accuracy limit, while δE_{tot} for Ni_2MnAl is negative (−0.94 meV/atom). These values of δE_{tot} indicate that the martensitic phase in Ni_2MnAl and Ni_2MnIn is not stable and so martensitic transition will not occur. This is in agreement with experimental data and earlier theoretical work.[15,16]

From the above data, a correlation emerges between δE_{tot} and T_M. Conceptually, this is understandable since larger δE_{tot} implies higher stability of the martensitic phase at zero temperature. A first-order transition to the austenitic phase would occur when with increasing temperature, the martensitic phase energy [defined by the energy minimum in Fig. 2(a)] would increase to reach the energy minimum for the austenitic phase. This means that with increasing temperature, to undergo transition to the austenitic phase, the energy of the martensitic phase has to overcome δE_{tot} and this would be directly related to $k_B T_M$. A similar concept has been used in Ref. 21 where, taking $\delta E_{tot} \propto k_B T_M$, the increase in T_M between Ni_2MnGa and $Ni_{2.25}MnGa$ could be explained. This expression should be generally valid and this indeed seems so for TiNi (45 and 333), TiPd (95 and 783), and TiPt (155 and 1343).[23] The numbers in parentheses indicate δE_{tot} and T_M in meV/atom and K, respectively, as taken from Ref. 23. Similar trend is obtained for Ni excess Ni-Mn-Ga.[21,24,28]

In Fig. 2(b), T_M versus δE_{tot} for all the shape memory alloys discussed above are plotted; T_M is taken to be zero for Ni_2MnIn and Ni_2MnAl. It is highly significant that although the theoretical data are from three different groups[20–24] on two different types of shape memory alloys and the methods of calculation are different, an approximately linear relation between T_M and δE_{tot} is evident. Thus the validity of the expression $\delta E_{tot} \propto k_B T_M$ is established. A rather good straight-line fit through the data for TiX (X=Ni, Pd, and Pt) (Ref. 23) is obtained [Fig. 2(b)]. Since the Ni-Mn-X (X=Ga, In, and Al) FSMAs are different from TiX, a separate straight line is fitted. The quality of the fit is similar to TiX except for data around 200 K. This is possibly because of the existence of modulated structures in this T_M range, which is not considered in theory. From the fitted line, T_M for Ga_2MnNi is estimated to be about 570 K (filled circle), corresponding to its δE_{tot}=55 meV [Fig. 2(b)].

It is generally believed that T_M would increase with the valence electron per atom ratio (e/a). However, this relation is of limited applicability and breaks down in many cases. For example, Ni_2MnGa, Ni_2MnIn, and Ni_2MnAl all have the same e/a (=7.75) but only Ni_2MnGa exhibits a martensitic transition. TiX (X=Ni, Pt, and Pd) has the same e/a (=6.5), but their T_M is very different. In Ni-Mn-Ga-In, although e/a is same, T_M changes.[9] For $Ni_{2-x}Mn_{1+x}Ga$ between $x=0.25$ and 1, we find that as e/a decreases from 7.31 to 6.75, T_M increases from 37 to 270 K.[13,30] For the alloys shown in Fig. 2(b), the absence of any correlation between T_M and e/a is shown as an inset. In contrast, the present approach explains all the above observations. For example, δE_{tot} decreases from 3.6 meV/atom to zero between Ni_2MnGa and Ni_2MnIn, which explains the decrease in T_M with In doping and the absence of a martensitic transition in Ni_2MnIn. Higher δE_{tot} in Mn_2NiGa rationalizes why its T_M is higher than Ni_2MnGa although its e/a (=6.75) is lower. Thus, the proportionality of T_M with δE_{tot} is of more general validity, since it has a theoretical foundation that involves all electron *ab initio* calculations unlike the phenomenological relation between T_M

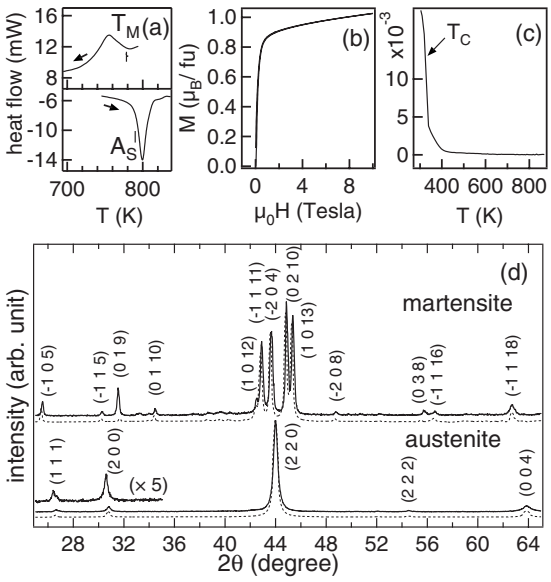

FIG. 3. (a) Differential scanning calorimetry showing the first-order martensitic transition. The transition temperatures are indicated by ticks, while the arrows show the heating and cooling directions. (b) Isothermal magnetization as a function of magnetic field at 2.5 K. (c) Magnetization as a function of temperature in low field (25 Oe). (d) X-ray diffraction pattern of Ga_2MnNi in the martensitic phase at room temperature (RT) and for the austenitic phase (recorded at RT after quenching the sample in ice water from 873 K). The simulated pattern (dashed line) is shifted along the vertical axis.

and e/a. In fact, this approach of determining the transition temperature should be applicable to any first-order structural transition.

B. Experimental studies

Differential scanning calorimetry on polycrystalline ingots of Ga_2MnNi shows a clear signature of a first-order martensitic transition with T_M=780 K and austenitic start temperature (A_s) of 790 K [Fig. 3(a)]. The experimental T_M is considerably higher than the theoretically predicted value, and a possible reason is discussed below. The latent heat of the transition turns out to be about 2.35 kJ/mol, which is similar to that reported for Ni excess Ni-Mn-Ga, for example, $Ni_{2.24}Mn_{0.75}Ga$.[28] The difference in the width of the heating and cooling thermograms could be related to the kinetics of the structural transition. EDAX measurements from different regions of $30\times30\mu^2$ area as well as the back scattered image show that the specimen is homogeneous. The average composition turns out to be $Ga_{1.9}Mn_{1.08}Ni_{1.02}$. In agreement with theory, the isothermal M-H curve at 2.5 K shows that Ga_2MnNi is indeed ferromagnetic [Fig. 3(b)]. The hysteresis loop is not clearly observed because the coercive field is small (≈25 mT). Such small coercive fields have been reported for other Ni-Mn-Ga alloys.[14,31] The saturation field is 1 T and the saturation moment is $1\mu_B$/f.u.. $M(T)$ at low field gives T_C=330 K [arrow, Fig. 3(c)]. This implies that the martensitic transition occurs in the paramagnetic state and expectedly $M(T)$ shows no change across T_M. If should be noted that the saturation moment of $1\mu_B$/f.u. is less than the theoretically calculated moment of about $3\mu_B$/f.u. The reasons for this disagreement could be that the actual sample has Mn excess, which might cause Mn clustering leading to antiferromagnetic coupling between Mn atom pairs as what has been observed for other Mn excess systems.[22,32,33] Moreover, note that the theory does not consider the actual monoclinic structure (discussed below) that might favor a different magnetic ground state with antiparallel coupling between Mn atoms.

The XRD pattern corresponding to the austenitic phase has been simulated by the Le Bail fitting procedure, and the structure is clearly cubic L_{2_1}. The relative intensity of the (200) peak compared to the (111) peak [shown in an expanded scale in Fig. 3(d)] confirms that the Ga atoms occupy the equivalent $8f$ position in agreement with theory (Fig. 1). The experimental lattice constant (a_{aus}=5.84 Å) is close to the calculated value (5.96 Å). However, the martensitic phase XRD pattern is more complicated than tetragonal and can be indexed by a monoclinic phase ($P2/m$ space group) with a=4.31, b=29.51, and c=5.55 Å and β=90.49°. Since $b\approx7a$, a seven-layer modulation may be expected, and such structures with monoclinic or orthorhombic symmetry that exhibit modulation have been reported for Ni-Mn-Ga.[34] Magnetic-field-induced strain has been observed in Ni-Mn-Ga for structures that exhibit modulation.[1] The c/a for this monoclinic cell (that can be compared to the theoretical c/a=0.83 for the tetragonal structure) is obtained by $c/a=5.55/(4.31\sqrt{2})=0.91$. Thus, the agreement between experimental and theoretical c/a is reasonable considering that a simplified structure is used in theory.

However, the most important point is that the experimental unit-cell volume of the martensitic phase is within 1% of that of a comparable austenitic cell given by $7a_{aus}^3/2$. This shows that the unit-cell volume hardly changes between the two phases, which is a necessary condition for a shape memory alloy. Thus, a unit-cell volume-conserving martensitic transition with small width of hysteresis [Fig. 3(a)] and presence of modulation indicate that Ga_2MnNi is indeed a FSMA material.

IV. CONCLUSION

The modulated martensitic structure of Ni-Mn-Ga is complicated and a controversy exists even about the structure of the well-studied Ni_2MnGa.[34] Atomic positions have not yet been determined for the monoclinic structure. Under such circumstances, our work is important because it shows that another FSMA material can be predicted by computing the energy cost of formation of the martensitic phase in a simpler tetragonal structure. The present work demonstrates that another FSMA material can be predicted by determining the energy stability of a tetragonal martensitic phase with respect to the cubic austenitic phase. This approach is successful because, although the modulated phase involves a large unit cell, the atoms are generally displaced only by a small amount from their positions compared to the tetragonal structure.[34] Since the tetragonal structure is not computationally demanding, precise calculations can be performed for

lattice-constant optimization in the lowest-energy magnetic state.[20–22] Thus, the total-energy difference can be determined with sufficient accuracy and T_M can be estimated. However, difference in T_M between experiment and theory could occur, as in this case, possibly because the latter does not consider the actual structure. In this context, it is to be noted (Fig. 2) that a subtle change in δE_{tot} can substantially alter the T_M value. Theory thus provides an important starting point for the experimentalists and experimental inputs can be used to further refine the theory. A direct proof of the FSMA behavior is the movement of twins with magnetic field and the actuation behavior. So, further work on the magnetomechanical behavior of Ga_2MnNi is in progress. Prediction of new materials in the quest for better properties is the need of the hour in FSMA research and the present work aims toward that.

ACKNOWLEDGMENTS

Help from the scientific computing group of the Computer Centre, RRCAT is acknowledged. I. Bhaumik, P. K. Mukhopadhyay, and R. J. Chaudhary are thanked for the useful discussions. Funding from Ramanna Research Grant, DST, and Max-Planck Partner Group Project is acknowledged.

*barman@csr.ernet.in

[1] S. J. Murray, M. Marioni, S. M. Allen, R. C. OHandley, and T. A. Lograsso, Appl. Phys. Lett. **77**, 886 (2000); A. Sozinov, A. A. Likhachev, N. Lanska, and K. Ullakko, *ibid.* **80**, 1746 (2002).

[2] J. Marcos, L. Mañosa, A. Planes, F. Casanova, X. Batlle, and A. Labarta, Phys. Rev. B **68**, 094401 (2003); X. Zhou, W. Li, H. P. Kunkel, and G. Williams, J. Phys.: Condens. Matter **16**, L39 (2004).

[3] C. Biswas, R. Rawat, and S. R. Barman, Appl. Phys. Lett. **86**, 202508 (2005).

[4] I. Takeuchi, O. O. Famodu, J. C. Read, M. A. Aronova, K.-S. Chang, C. Craciunescu, S. E. Lofland, M. Wuttig, F. C. Wellstood, L. Knauss, and A. Orozco, Nature Mater. **2**, 180 (2003).

[5] T. Krenke, E. Duman, M. Acet, E. F. Wassermann, X. Moya, L. Mañosa, and A. Planes, Nature Mater. **4**, 450 (2005).

[6] R. Kainuma, Y. Imano, W. Ito, Y. Sutou, H. Morito, S. Okamoto, O. Kitakami, K. Oikawa, A. Fujita, T. Kanomata, and K. Ishida, Nature (London) **439**, 957 (2006).

[7] Y. Sutou, Y. Imano, N. Koeda, T. Omori, R. Kainuma, K. Ishida, and K. Oikawa, Appl. Phys. Lett. **85**, 4358 (2004).

[8] T. Krenke, M. Acet, E. F. Wassermann, X. Moya, L. Mañosa, and A. Planes, Phys. Rev. B **73**, 174413 (2006).

[9] M. Khan, I. Dubenko, S. Stadler, and N. Ali, J. Phys.: Condens. Matter **16**, 5259 (2004).

[10] A. T. Zayak, P. Entel, K. M. Rabe, W. A. Adeagbo, and M. Acet, Phys. Rev. B **72**, 054113 (2005).

[11] A. N. Vasil'ev, A. D. Bozhko, V. V. Khovailo, I. E. Dikshtein, V. G. Shavrov, V. D. Buchelnikov, M. Matsumoto, S. Suzuki, T. Takagi, and J. Tani, Phys. Rev. B **59**, 1113 (1999).

[12] V. V. Khovaylo, V. D. Buchelnikov, R. Kainuma, V. V. Koledov, M. Ohtsuka, V. G. Shavrov, T. Takagi, S. V. Taskaev, and A. N. Vasiliev, Phys. Rev. B **72**, 224408 (2005).

[13] G. D. Liu, J. L. Chen, Z. H. Liu, X. F. Dai, G. H. Wu, B. Zhang, and X. X. Zhang, Appl. Phys. Lett. **87**, 262504 (2005).

[14] S. Banik, A. Chakrabarti, U. Kumar, P. K. Mukhopadhyay, A. M. Awasthi, R. Ranjan, J. Schneider, B. L. Ahuja, and S. R. Barman, Phys. Rev. B **74**, 085110 (2006).

[15] A. Ayuela, J. Enkovaara, K. Ullakko, and R. M. Nieminen, J. Phys.: Condens. Matter **11**, 2017 (1999).

[16] V. V. Godlevsky and K. M. Rabe, Phys. Rev. B **63**, 134407 (2001).

[17] A. Ayuela, J. Enkovaara, and R. M. Nieminen, J. Phys.: Condens. Matter **14**, 5325 (2002).

[18] C. Bungaro, K. M. Rabe, and A. Dal Corso, Phys. Rev. B **68**, 134104 (2003); J. M. MacLaren, J. Appl. Phys. **91**, 7801 (2002).

[19] A. T. Zayak, P. Entel, J. Enkovaara, and R. M. Nieminen, J. Phys.: Condens. Matter **15**, 159 (2003).

[20] S. R. Barman, S. Banik, and A. Chakrabarti, Phys. Rev. B **72**, 184410 (2005).

[21] A. Chakrabarti, C. Biswas, S. Banik, R. S. Dhaka, A. K. Shukla, and S. R. Barman, Phys. Rev. B **72**, 073103 (2005).

[22] S. R. Barman, S. Banik, A. K. Shukla, C. Kamal, and A. Chakrabarti, Europhys. Lett. **80**, 57002 (2007); S. R. Barman and A. Chakrabarti, Phys. Rev. B **77**, 176401 (2008).

[23] Y. Y. Ye, C. T. Chan, and K. M. Ho, Phys. Rev. B **56**, 3678 (1997).

[24] J. Chen, Y. Li, J. Shang, and H. Xu, Appl. Phys. Lett. **89**, 231921 (2006).

[25] K. Bhattacharya, *Microstructure of Martensite* (Oxford University Press, Oxford, 2003).

[26] P. Blaha, K. Schwartz, and J. Luitz, *WIEN97, A Full Potential Linearized Augmented Plane Wave Package for Calculating Crystal Properties* (Karlheinz Schwarz, Technology Universität, Wien, Austria, 1999).

[27] M. Weinert, E. Wimmer, and A. J. Freeman, Phys. Rev. B **26**, 4571 (1982).

[28] S. Banik, R. Ranjan, A. Chakrabarti, S. Bhardwaj, N. P. Lalla, A. M. Awasthi, V. Sathe, D. M. Phase, P. K. Mukhopadhyay, D. Pandey, and S. R. Barman, Phys. Rev. B **75**, 104107 (2007).

[29] K. W. Kim, Y. V. Kudryavtsev, J. Y. Rhee, N. N. Lee, and Y. P. Lee, IEEE Trans. Magn. **40**, 2775 (2004).

[30] S. Banik, R. Rawat, P. K. Mukhopadhyay, B. L. Ahuja, A. M. Awasthi, S. R. Barman, and E. V. Sampathkumaran (unpublished).

[31] R. Tickle and R. D. James, J. Magn. Magn. Mater. **195**, 627 (1999).

[32] J. Enkovaara, O. Heczko, A. Ayuela, and R. M. Nieminen, Phys. Rev. B **67**, 212405 (2003).

[33] S. Banik, R. Rawat, P. K. Mukhopadhyay, B. L. Ahuja, Aparna Chakrabarti, P. L. Paulose, Sanjay Singh, Akhilesh Kumar Singh, D. Pandey, and S. R. Barman, Phys. Rev. B **77**, 224417 (2008).

[34] P. J. Brown, J. Crangle, T. Kanomata, M. Matsumoto, K.-U. Neumann, B. Ouladdiaf, and K. R. A. Ziebeck, J. Phys.: Condens. Matter **14**, 10159 (2002); J. Pons, R. Santamarta, V. A.

Chernenko, and E. Cesari, J. Appl. Phys. **97**, 083516 (2005); R. Ranjan, S. Banik, S. R. Barman, U. Kumar, P. K. Mukhopadhyay, and D. Pandey, Phys. Rev. B **74**, 224443 (2006); Y. Ge, A. Sozinov, O. Söderberg, N. Lanska, K. Ullakko, and V. K. Lindroos, J. Phys. IV **112**, 921 (2003); L. Righi, F. Albertini, L. Pareti, A. Paoluzi, and G. Calestani, Acta Mater. **55**, 5237 (2007).